Research and Reports in Urology

Dovepress
Taylor & Francis Group

Open Access Full Text Article

ORIGINAL RESEARCH

As a New Tumor Suppressor Gene, PID1 Activates the AMPK-mTOR Signal to Inhibit the Progression of Bladder Cancer

Lingfeng Sun[1–3], Chengyi Liu[3], Yu Cao[4], Jianghao Li[1,2], Lin Yuan[1,2]

[1]The First Clinical Medical College, Nanjing University of Chinese Medicine, Nanjing, Jiangsu, People's Republic of China; [2]Department of Urology, Affiliated Hospital of Nanjing University of Chinese Medicine, Jiangsu Province Hospital of Chinese Medicine, Nanjing, Jiangsu, People's Republic of China; [3]Department of Urology Department of Urology, LU'AN Hospital of Anhui Medical University, Lu'an, Anhui, People's Republic of China; [4]Department of Dermatology, The First Clinical Medical College, The First Affiliated Hospital of Anhui University of Chinese Medicine, Hefei, Anhui, People's Republic of China

Correspondence: Lin Yuan, Department of Urology, Affiliated Hospital of Nanjing University of Chinese Medicine, Jiangsu Province Hospital of Chinese Medicine, Nanjing, Jiangsu, People's Republic of China, Tel +86-025-86617141, Email yuanlin47@126.com

Purpose: Bladder cancer is one of the ten most common cancers in the world, with a high incidence rate and mortality, and therefore a major burden on the global health care system. PID1 (Phosphotyrosine Interaction Domain 1) functions as an intracellular receptor protein for LRP1. The purpose of this study was to explore the role of PID1 in bladder cancer.

Methods: RNA-seq data analysis was conducted on 404 BLCA specimens and 28 normal specimens to identify differentially expressed genes. The findings indicated a strong correlation between PID1 expression levels and bladder cancer. We constructed a bladder cancer cell line stably overexpressing PID1 and assessed its impact on cell proliferation and migration. Additionally, We used RT-112 cells to induce tumor formation in nude mice to study the function of the *PID1* gene in vivo.

Results: PID1 expression was notably low in bladder cancer tissues. Compared to SV-HUC-1, RT-112, and SCaBER bladder cells exhibited significantly reduced PID1 expression. Overexpressing PID1 in cells led to the promotion of apoptosis in bladder cancer cells and suppressed cell proliferation and metastasis. In vivo, the overexpression of PID1 demonstrated a significant inhibitory effect on bladder cancer. Furthermore, it was capable of activating the AMPK-mTOR signaling pathway, thereby inhibiting tumor progression.

Conclusion: PID1 exhibits a potent inhibitory effect on bladder cancer and activates the AMPK-mTOR signaling pathway to hinder tumor growth.

Keywords: bladder cancer, PID1, AMPK, mTOR

Introduction

Bladder cancer is one of the most common malignant tumors of the urinary system, with the main onset age between 50 and 70 years old. Bladder cancer can be divided into non-muscular invasive and invasive.[1] Non-invasive urothelial carcinoma is usually confined to the bladder mucosa and has a relatively good prognosis;[2] However, invasive urothelial carcinoma can invade the bladder muscle layer and even extra bladder tissue, with a high risk of metastasis.[3] The 5-year survival rate may only be 30–50%, and the prognosis is poor. NMIBC often recurs or progresses, with five-year incidence rates of 31–78% and 1–45%, respectively.[4] The direct and indirect cost of diagnosis and treatment of bladder cancer is currently the highest among all elderly malignant tumors, with an annual direct and indirect loss of nearly $4 billion.[5] The common risk factors of bladder cancer were smoking, age, and occupational exposure.[6] The treatment of non-muscular invasive bladder cancer is mainly transurethral resection of bladder tumor (TURBT) and chemotherapy; The treatment of myometrial invasive bladder cancer requires further radical cystectomy or triple therapy TMT.[1] Despite undergoing relevant treatments, 72.2% of patients still experience recurrence, progress, or die of bladder cancer.[7] Early detection, recurrence monitoring, and diagnostic methods of bladder cancer, such as urine DNA methylation analysis[8] and Ultra Deep Sequencing of Plasma Cell-

Received: 24 March 2025
Accepted: 12 July 2025
Published: 24 July 2025

Free DNA[9] can also improve the prognosis of BCA patients. Exploring the molecular mechanism of bladder cancer carcinogenesis and the cause of high recurrence is essential for the treatment of bladder cancer.

PID1 (Phosphotyrosine interaction domain containing 1) is a protein containing a phosphotyrosine interaction domain,[10] it plays a role in intracellular signal transduction,[11] energy metabolism regulation,[12] and other processes. PID1 was initially found to be associated with metabolic diseases such as obesity and insulin resistance.[13] The *PID1* gene is highly expressed in the adipose tissue of obese patients and can reduce insulin uptake of glucose, and it can promote the proliferation and differentiation of adipocytes and enhance obesity-related insulin resistance.[14] As more and more studies have shown, PID1 plays an anti-cancer role in glioma[15] and liver cancer.[16] PID1 is significantly downregulated in patients with chronic obstructive pulmonary disease caused by smoking.[17] Smoking is also an important independent risk factor for bladder cancer.[18] At present, the relationship between PID1 and bladder cancer has not been reported.

Materials and Methods

Clinical Sample Immunohistochemistry (IHC)

A total of 10 bladder cancer tissue samples from May 2024 to October 2024 were collected. All samples were approved by Lu'an Hospital, Anhui Medical University (Ethical approval No.2025 LLKS-KY-014). All patients signed informed consent and complied with the Declaration of Helsinki. The received samples were fixed in 4% polyformaldehyde (BL539A, Biosharp, Beijing, China) for 24 hours, followed by dehydration, paraffin embedding, and sectioning. For immunohistochemical detection of PID1 protein expression, the sections were dewaxed, treated with a pH6.0 citric acid solution to repair antigens, blocked peroxidase with endogenous peroxidase inhibitors, and sealed with an immunoprecipitation buffer. The PID1 antibody (bs-8065, Bioss, Beijing, China) was diluted 1:50 in the antibody dilution solution and incubated overnight at 4°C. The IgG-HRP Robbit (SA00001-2, Proteintech, Wuhan, China) was diluted 1:200 in the antibody dilution solution and incubated in the dark for 4 hours. DAB staining was performed, followed by hematoxylin re-staining of the cell nuclei, dehydration, and mounting. The samples were then photographed under an inverted microscope.

Cell Culture

HEK-293T cells were provided by the Chinese Academy of Sciences Cell Bank, and SV-HUC-1, RT-112, and SCaBER cells were purchased from Wuhan Pusen Life Science Co., Ltd. The complete medium was prepared by adding 10% fetal bovine serum (10099141C, Gibco, USA) and 1% penicillin-streptomycin double antibody (15240–062, Gibco, USA) to the basic culture medium. The culture conditions are 37°C, 95% air, and 5% CO_2.

Stable Overexpression Cell Line Construction

The PID1 overexpression plasmid was constructed using the lentiviral expression vector pLV3-CMV-MCS-3FLAG-PURO (Limibio, Biotechnology Co., Ltd. China), pMD2.G Addgene, USA) and the psPAX 2 (12260, Addgene, USA) lentiviral packaging system. The 293T cells were transfected with Lipofectamine_2000 (11668–019, Invitrogen, USA). After 48 hours, the PID1 lentivirus was collected. RT-112 and SCaBER cells were infected with pLV3-NC and pLV3-PID1 lentiviruses for 2 days, respectively. The cells were then selectively transfected with puromycin (1000 ng/mL). The expression of the *PID1* gene was detected using RT-qPCR and Western blotting.

CCK-8 Assay

Cells were evenly distributed at a density of 1×10^4 cells per well in a 96-well plate. The cells were cultured for 48 hours in an environment with 37°C, 95% air, and 5% CO_2. The 100X CCK-8 reagent (BS350A, Biosharp, Beijing, China) was diluted into the medium to achieve a 1X concentration. Each well contained 110 μL of the diluted CCK-8 solution, and the cells were incubated in a cell culture incubator for 2 hours. The absorbance was measured using a multi-functional ELISA (Biotek, SYNERGY HTX, VT, USA) at 450 nm.

Cell Migration and Invasion Detection

Cells are inoculated into a 6-well plate. Once the cells have fully grown, a micro-pipette is used to create a scratch and the culture medium is changed. The plate is then imaged using a microscope imaging system. After 48 hours of cultivation, the plate is imaged again to analyze cell migration rates. For transwell assays, cells are inoculated into a transwell plate. In the lower chamber, 1mL of complete medium is added, and in the upper chamber, 0.5mL of a cell suspension mixed with serum-free medium is added, with a density of $1\times10_3$ cells/mL. After 48 hours of cultivation, the medium is discarded from the plate, and the plate is washed with PBS. The cells are then fixed with 4% polyformaldehyde for 2 hours, followed by a PBS wash. The cells are stained with 0.1% crystal violet (BL802A, Biosharp, Beijing, China) for 10 minutes, and the excess dye is removed by two PBS washes. Finally, the plate is inverted and imaged under a microscope.

Flow Cytometry Analysis

The collection of cells was performed according to the instructions provided in the AnnexinV-FITC/PI double staining cell apoptosis detection kit (BL107A, Biosharp, Beijing, China) and the cell cycle and apoptosis detection kit (BL114A, Biosharp, Beijing, China). This process involves detecting cell apoptosis and cell cycle. After 48 hours of cell culture, the cells were collected and labeled. The cells were first washed twice with pre-cooled PBS, then resuspended in 500 μL of binding buffer. The staining reagents were added according to the kit instructions, and the samples were incubated in the dark at room temperature for 15 minutes. The cell ratios in each sample were analyzed using a flow cytometer (CytoFLEX, Beckman, USA), and the data was analyzed using CytExpert 2.4 software.

RT-qPCR

Using TRIzolReagent (15596–026CN, Invitrogen, USA), RNA was extracted from the cells. Then, cDNA was synthesized using the Hifair II First-Chain cDNA Synthesis Kit (11139ES10, YEASEN, Shanghai, China). A Real-time PCR amplification system was set up using the Universal Fluorescent Quantitative PCR Kit (BL697A, Biosharp, Beijing, China). The gene primers are listed in Table 1. PCR detection was performed using the LightCycler 96 PCR System (Roche, Swiss Confederation).

Western Blot

Proteins were separated by SDS-PAGE and sealed with 5% skim milk for 2 hours. The primary antibody was diluted at a ratio of 1:1000 and incubated overnight at 4 °C. After washing the membrane with TBS, the secondary antibody was diluted at a ratio of 1:10000 and incubated at room temperature for 1 hour. The immunoblot was imaged using the Tanon 5200 chemiluminescence imaging system (Tanon, Wuhan, China). PID1 (bs-8065 R) was purchased from Boss (Beijing, China), AMPK α (AF 6423), p-AMPK α (AF 3423), mTOR (AF 6308), p-mTOR (AF 3308), and Beclin 1 (AF 5128) were purchased from Affinity (Shanghai, China), Caspase 3 (R23727) was purchased from Zenbio (Sichuan, China), and E-cadherin (20874-1-AP), N-cadherin (22018-1-AP), vimentin (10366-1-AP) and GAPDH (60004-1-IG) were purchased from Proteintech (Wuhan, China). The gray values were analyzed using MBF_Image J.

RNA-Seq

Use Truseq RNA library preparation kit v2 (Illumina, USA) for library construction. In Illumina Novaseq ™ Perform multiplex analysis and sequencing on the sample library using a paired read length of 250bp on the 6000 platform (Illumina). Each sample generated an average of 6G clean data and commissioned LC Bio-Technology CO., Ltd.

Table 1 Tumor Weight, Tumor Volume, and Tumor Inhibition Rate in Nude Mice ($\bar{x}$ ±s, n=5)

Group	Body Weight (g)	Tumor Weight (g)	Tumor Volume (mm^3)	Inhibition Rate (%)
Blank	30.11±1.25	0.31±0.13	386.20±106.79	–
OE-NC	30.34±1.25	0.32±0.11	372.54±126.52	-
PID1-OE	29.52±0.93	0.19±0.32**	188.30±42.26*	46.45±11.34

Notes: Compared to the NC group, **P<0.01, * P<0.05.

https://doi.org/10.2147/RRU.S530209

(Hangzhou, China) for bioinformatics analysis. The analysis was conducted using edgeR software to analyze the significance of expression differences. The threshold for screening differentially expressed genes, | log2FC |>2 and padj<0.05, were used as the criteria for significant differences.

Tumor Formation Experiment in vivo

All animal procedures were approved by the laboratory of Nanjing University of Chinese Medicine (Ethical Approval No. LLSC 20242215) and adhered to the 3R principles of animal ethics. 24 BALB/c nude mice, SPF grade, aged around 5–6 weeks, male. Purchased from Henan Scribes Biotechnology Co., Ltd. [Experimental Animal Production License No. SCXK (Yu) 2020–0005], with a feeding environment temperature of (23 ± 2) °C and relative humidity of (60 ± 10)%, free to eat and drink water. The drinking water is sterilized grade II ultrapure water, and the quality of the drinking water meets the requirements of the national standard "Sanitary Standards for Drinking Water" (GB5749-2006) of the People's Republic of China. Adapt to the animal room environment for one week before the experiment. After the injection of cancer cells, the tumor volume was regularly monitored. Tumor samples were collected 27 days post-surgery, weighed, photographed, and recorded.

Statistical Analysis

Use GraphPad Prism (GraphPad, USA) software to evaluate statistical significance. The data is displayed as mean in SEM ±. Student's *t*-test is used to compare data between two groups, while analysis of variance is used to analyze differences between three or more groups. P<0.05 is used as the standard for statistical significance.

Results

PID1 Is Low in Bladder Cancer Tissue and Bladder Cancer Cells

We analyzed the top 100 differentially expressed genes in 36 cases of UCB and 29 adjacent normal bladder tissues from the GEO dataset GSE133624 and identified 32 differentially expressed genes (Figure 1A) by intersecting these with the top 250 differentially expressed genes in basal-like bladder cancer (BLCA). Using the Gepia website (http://gepia2.cancer-pku.cn, we conducted a preliminary evaluation of these genes and found that *PID1* was significantly down-regulated in BLCA patients (Figure 1B). Relationship between *PID1* expression and overall survival rate of cancer patients (Figure 1C). It showed that the expression level of *PID1* was significantly related to the survival time of cancer patients. Immunohistochemical analysis of clinical samples showed that PID1 expression in bladder cancer tissue was significantly lower than in paracancerous tissue (P<0.001) (Figure 1D). In immortalized human ureteral epithelial cells SV-HUC-1, the mRNA level of PID1 was significantly higher than in human bladder cancer cells RT-112 and human bladder squamous cell carcinoma cells SCaBER (P<0.01) (Figure 1E). The protein expression levels of PID1 in RT-112 and SCaBER were also significantly lower than in SV-HUC-1 (P<0.01) (Figure 1F).

PID1 Inhibits the Proliferation of Cancer Cells and Promotes the Apoptosis of Cancer Cells

The overexpression plasmid of the *PID1* gene was constructed and subjected to Sanger sequencing (see Attachment 1). Stable cell lines overexpressing PID1 were established in RT-112 and SCaBER cells, and the expression of PID1 in these cells was detected using quantitative PCR and Western blotting (Figure 2A). This indicates the successful construction of stable overexpression cell lines for PID1. CCK-8 assay demonstrated that overexpression of PID1 significantly inhibited the proliferation of RT-112 and SCaBER cells, with an inhibition rate exceeding 20% (Figure 2B). Flow cytometry analysis of apoptosis and cell cycle progression revealed that overexpression of PID1 significantly promoted apoptosis in RT-112 and SCaBER cells (Figure 2C). After overexpression of PID1, the number of G1 phase cells in RT-112 and SCaBER cells decreased significantly, while the number of S phase cells increased markedly, indicating that over-expression of PID1 arrested RT-112 and SCaBER cells in the S phase (Figure 2D).

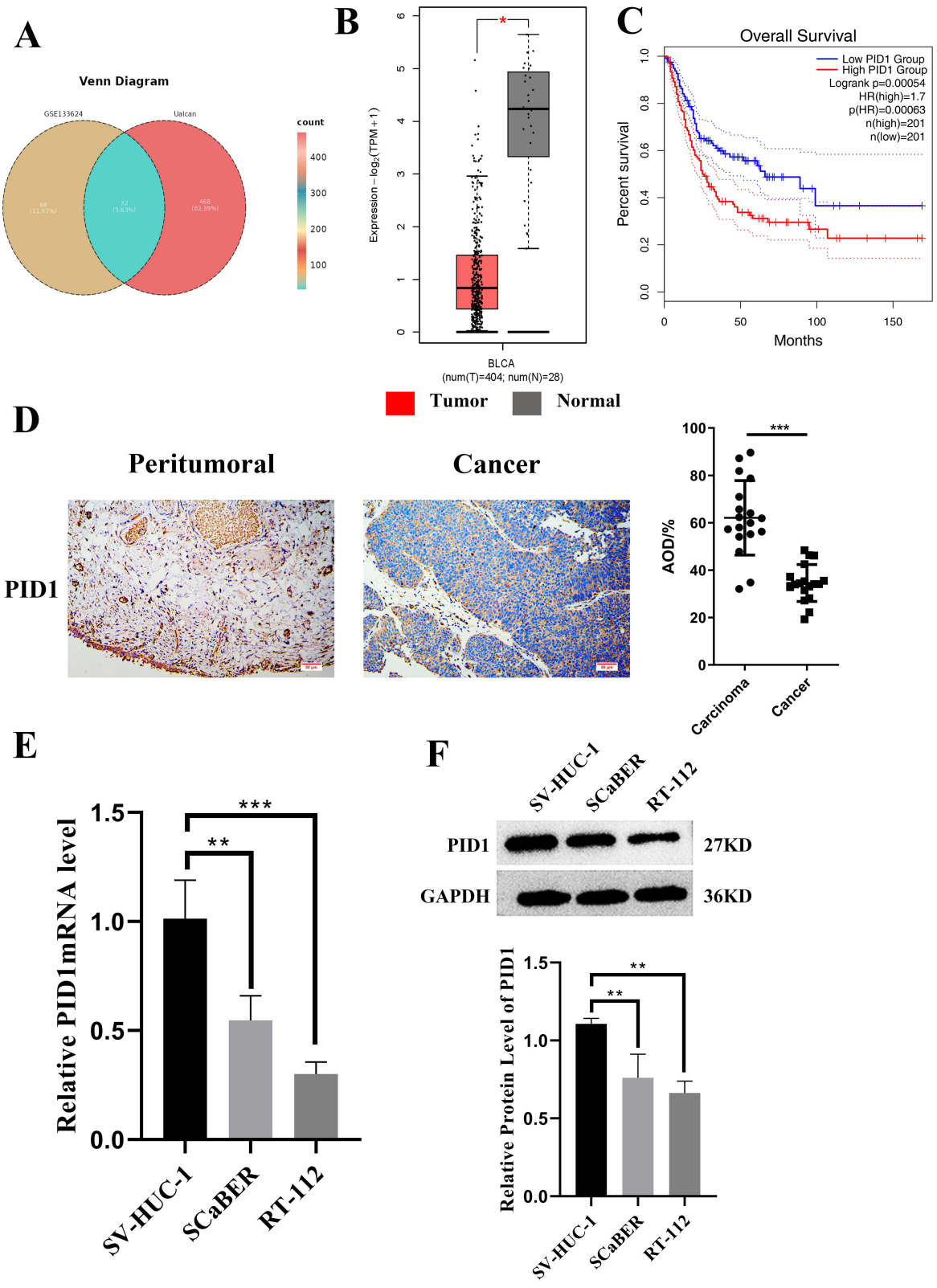

Figure 1 PID1 is low in bladder cancer tissue and bladder cancer cells. (**A**) The Venn Diagram of GSE133624 and top 250 genes by Ualcan. (**B**) Box plot of *PID1* expression analysis between bladder cancer and normal samples by GEPIA2 website (* $P < 0.05$, versus normal group). (**C**) Relationship between PID1 expression and overall survival rate of cancer patients by GEPIA2 website. (**D**) IHC staining of PID1 protein in clinical bladder cancer tissue samples (200X), The expression of PID1 in bladder cancer tissue was significantly lower than that in paracancerous tissue (n=10, *** $P<0.001$ versus paracancerous group). (**E**) Compared with SV-HUC-1 cells, the expression of the *PID1* gene was significantly reduced in RT-112 and SCaBER cells (n=3, ** $P<0.01$, *** $P<0.001$ versus SV-HUC-1 group). (**F**) The expression of PID1 protein in each cell was checked by Western Blot, The expression of PID1 protein in SCaBER and RT-112 cells compared with SV-HUC-1 cells (n=3, ** $P<0.01$ versus SV-HUC-1 group).

https://doi.org/10.2147/RRU.S530209

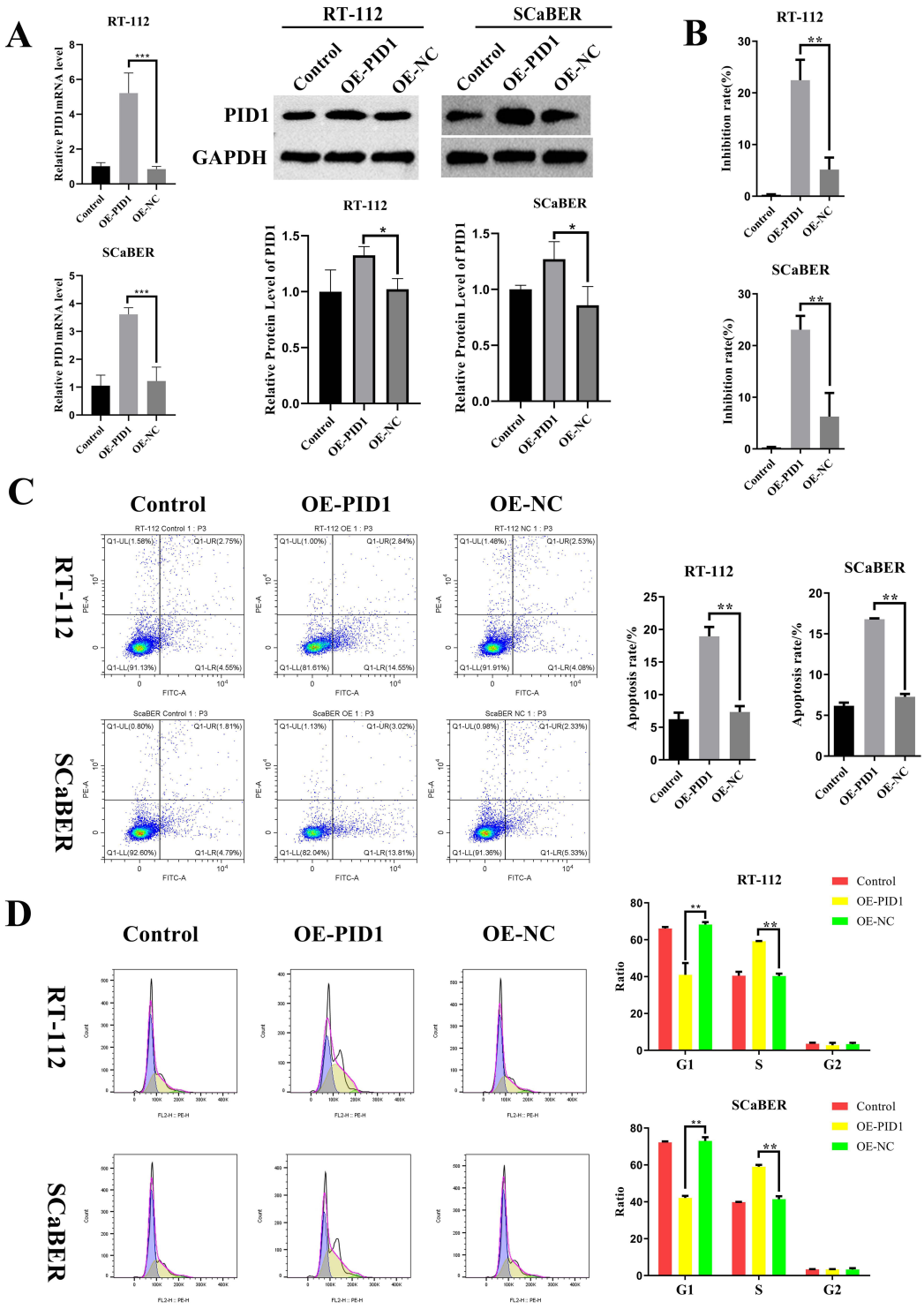

Figure 2 PID1 inhibits the proliferation of cancer cells and promotes the apoptosis of cancer cells. (**A**) Expression levels of PID1 mRNA in stable transfection cell lines overexpressing PID1. The expression levels of PID1 mRNA were significantly increased in the OE-PID1 group of RT-112 and SCaBER (n=3, *** P<0.001 versus the OE-NC group). Expression levels of PID1 protein in PID1 overexpression stable cell lines. The expression levels of PID1 protein were significantly increased in the OE-PID1 group of RT-112 and SCaBER (n=3, * P<0.05 versus the OE-NC group). (**B**) CCK8 assay was used to detect the inhibitory effect of PID1 overexpression on RT-112 and SCaBER cells, and the inhibitory rate of OE-PID1 group in RT-112 and SCaBER was significantly increased (n=3, ** P<0.01 versus OE-NC group). (**C**) The apoptosis effect of flow detection of PID1 overexpression on RT-112 and SCaBER cells was observed, and the apoptosis rate in the OE-PID1 group of RT-112 and SCaBER was significantly increased (n=3, ** P<0.01 versus OE-NC group). (**D**) The effect of overexpression of PID1 on the cell cycle of RT-112 and SCaBER cells was investigated by flow cytometry. In RT-112 and SCaBER, the G1 phase was significantly reduced and the S phase rate was significantly increased in the OE-PID1 group (n=3, ** P<0.01 versus the OE-NC group).

https://doi.org/10.2147/RRU.S530209

PID1 Inhibits the Migration, Invasion, and EMT Progression of Cancer Cells

The cell scratch assay was used to assess cell migration. The 48-hour migration rate of RT-112 cells was approximately 23%, and this rate decreased to about 5% after overexpression of the *PID1* gene. For SCaBER cells, the 48-hour migration rate was around 32%, and this rate dropped to about 18% after overexpression of the *PID1* gene. These results indicate that overexpression of PID1 significantly inhibits the migration of both RT-112 and SCaBER cells (Figure 3A). The Transwell chamber assay and the cell scratch assay yielded consistent results, showing a significant reduction in the invasion rate of RT-112 and SCaBER cells after overexpression of PID1. Specifically, the invasion rate of RT-112 cells was approximately 68% after overexpression of the *PID1* gene, and for SCaBER cells, it was approximately 64% (Figure 3B). Western blotting was performed to detect the expression levels of E-cadherin, N-cadherin, and cadherin in RT-112 and SCaBER cells. Overexpression of PID1 led to an increase in the level of E-cadherin in RT-112 cells ($P<0.05$), while the levels of N-cadherin and cadherin decreased slightly ($P<0.05$) (Figure 3C). In SCaBER cells, the level of E-cadherin increased significantly ($P<0.05$), while the levels of N-cadherin and Vimentin decreased ($P<0.05$) (Figure 3C).

PID1 Inhibited the Proliferation of Bladder Cancer Cells in Mice

We examined the tumorigenicity of the blank strain, overexpression control strain, and stably overexpressed PID1 transgenic strain in RT-112 cells. In vivo imaging revealed that the fluorescence signal in the PID1-OE group was significantly weaker compared to the overexpression control group (Figure 4A). The tumor comparison chart clearly shows the changes in tumor size and volume in the PID1 group, with the tumors in the PID1 overexpression group being notably smaller (Figure 4B). After 27 days of tumorigenicity, the mice's body weight was approximately 30 g, and there was no statistically significant difference between the groups ($P>0.05$) (Figure 4C). There was no significant difference in tumor volume and weight between the blank group and the overexpression control group compared to the overexpression control group ($P>0.05$), while the PID1 overexpression group showed a significant reduction in tumor volume and weight ($P<0.05$) (Figure 4D and E). The tumor inhibition rate based on tumor volume was 40.62%, and the tumor inhibition rate based on tumor weight was 49.54%.

Detection of PID1-Mediated Differential Gene Expression in Bladder Cancer by RNA Sequencing

To explore the molecular mechanisms by which PID1 inhibits bladder cancer, we analyzed the RNA sequences of the PID1 overexpressed RT-112 cell line and the control overexpressed RT-112 cell line. We identified 1,713 upregulated genes and 2,143 downregulated genes. The volcano plot shows good intra-group reproducibility of the samples, with significant differences between the overexpression group and the control group. PID1 further reduced gene expression (Figure 5B). In terms of GO terms, the upregulation was mainly in signal transduction, apoptosis processes, and inflammatory responses (Figure 5C), while the downregulation was primarily in cell adhesion, cell division, and cell migration (Figure 5D). The KEGG pathway analysis highlighted pathways closely associated with tumors, such as the AMPK signaling pathway and the PI3K-Akt signaling pathway, while pathways like the Wnt signaling and the ECM receptor interaction were downregulated (Figure 5E).

PID1 Regulates the Downstream AMPK/mTOR Pathway

To verify the AMPK pathway in tumor tissues, we conducted PCR analysis on *AMPKα, mTOR, Wnt5a, β-catenin*, and the apoptosis-related protein *Caspase 3* and the autophagy-related protein *Beclin 1* (Figure 6A). The results showed that *AMPKα, Caspase 3*, and *Beclin 1* were significantly upregulated ($P<0.05$), while *mTOR* and *Wnt5a* were significantly downregulated ($P<0.05$). Additionally, we performed Western Blot analysis on several proteins in the AMPK/mTOR pathway (Figure 6B). Compared to the control group, the overexpression of PID1 significantly increased AMPKα, p-AMPKα, Caspase 3, and Beclin 1 ($P<0.01$), while mTOR showed a downward trend but no significant difference ($P>0.05$), and p-mTOR was significantly decreased ($P<0.01$).

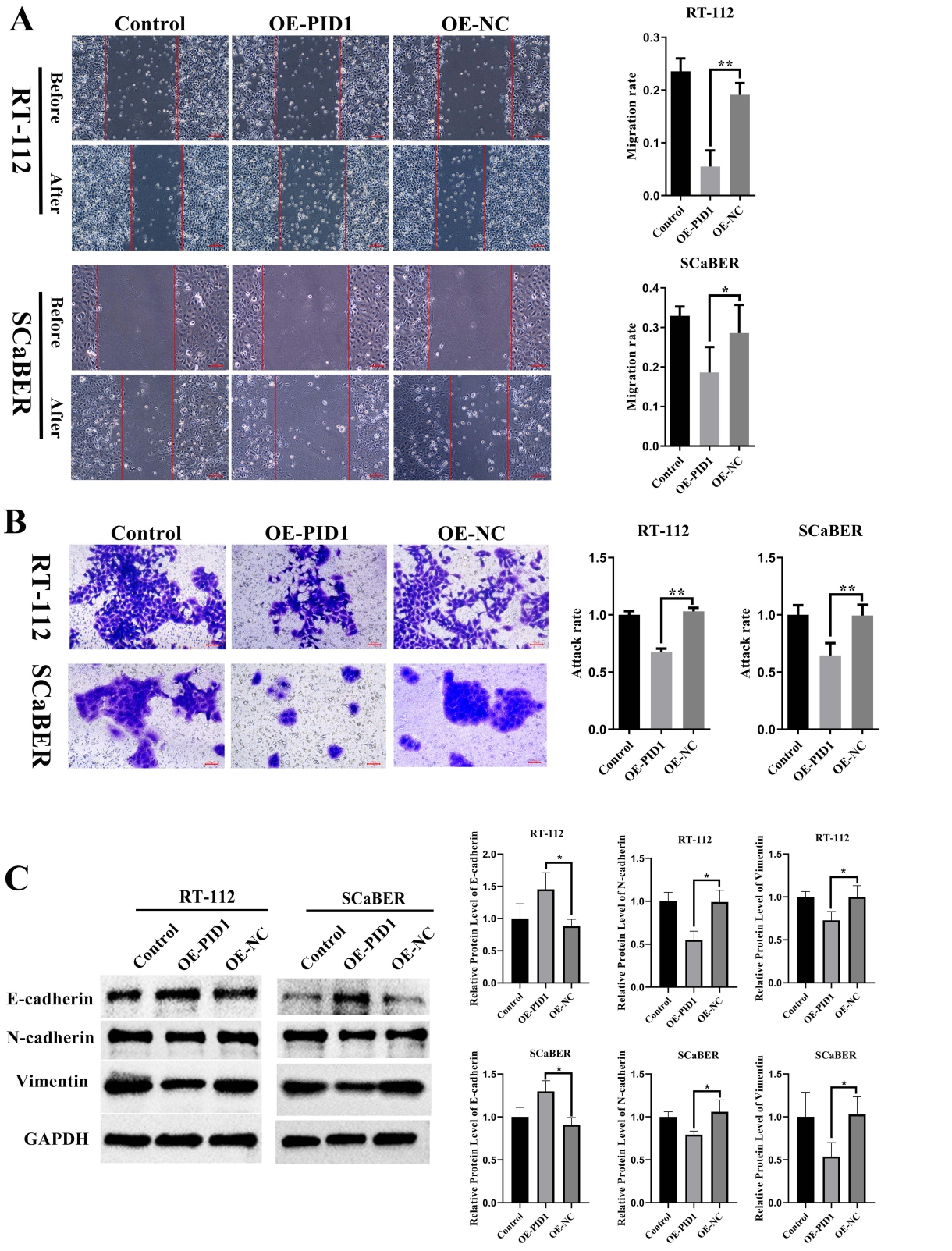

Figure 3 PID1 inhibits the migration, invasion, and EMT progression of cancer cells. (**A**) The cell scratch assay was used to detect the effect of PID1 overexpression on cell migration in RT-112 and SCaBER cells, and the migration rate of the OE-PID1 group in RT-112 and SCaBER was significantly reduced (n=3, **P*<0.05, ***P*<0.01 versus OE-NC group). (**B**) The transwell cell chamber assay was used to detect the effect of PID1 overexpression on the invasion of RT-112 and SCaBER cells, and the invasion rate of the OE-PID1 group in RT-112 and SCaBER was significantly reduced (n=3, ***P*<0.01 versus OE-NC group). (**C**) Western blot was used to detect the EMT effect of PID1 overexpression on RT-112 and SCaBER cells. The levels of EMT marker protein, E-cadherin, were significantly increased in the OE-PID1 group of RT-112 and SCaBER, while the expression levels of N-cadherin and Vimentin were decreased (n=3, **P*<0.05 versus OE-NC group).

https://doi.org/10.2147/RRU.S530209

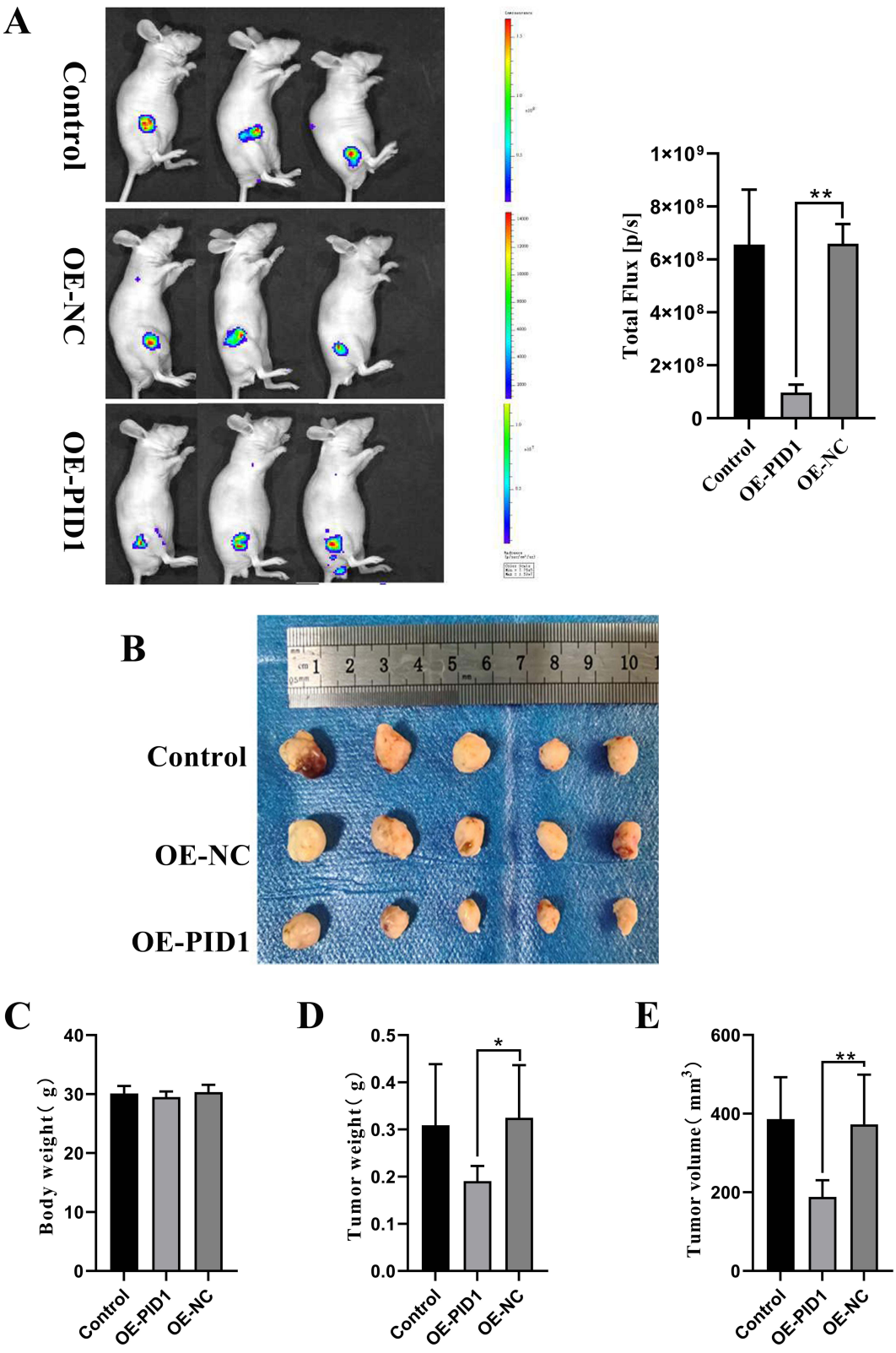

Figure 4 PID1 inhibits the proliferation of bladder cancer cells in mice. (**A**) Live fluorescence imaging of animals in each group. Fluorescence brightness analysis of in vivo tumor formation imaging in various animal groups (n=3, ***P*<0.01 versus OE-NC group). (**B**) Tumor images of dissected animals in each group. (**C**) Comparative analysis of body weight of mice in different groups after tumor formation. (**D**) Comparative analysis of tumor weight after tumor formation in different groups of mice (n=6, * *P*<0.05 versus OE-NC group). (**E**) Comparative analysis of tumor volume after tumor formation in different groups of mice (n=6, ** *P*<0.01 versus OE-NC group).

https://doi.org/10.2147/RRU.S530209

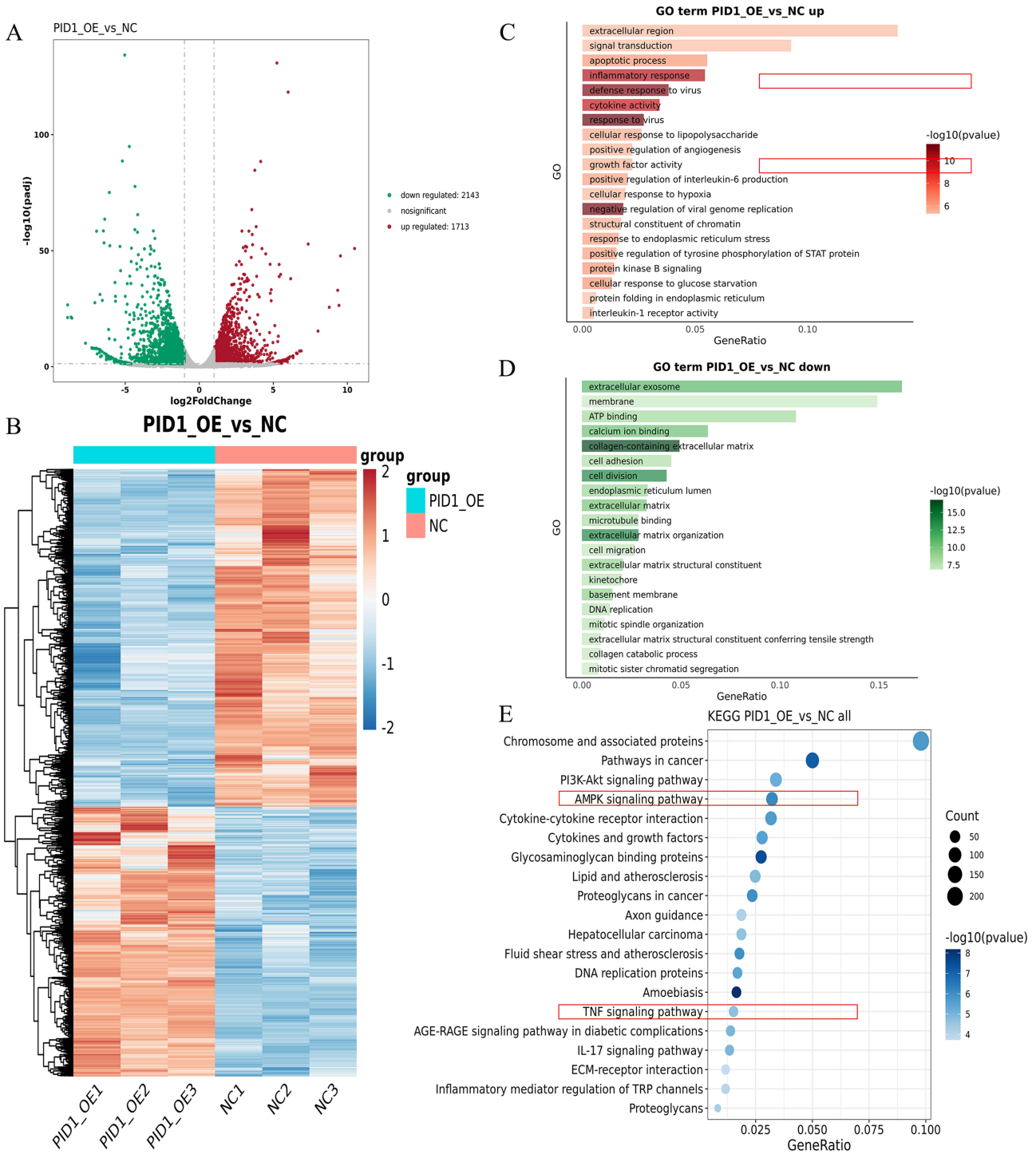

Figure 5 Detection of PID1 mediated differential gene expression in bladder cancer by RNA sequencing. (**A**) Volcanic diagram analysis of downstream gene expression by PID1 overexpression (Threshold: FC>2, *P*<0.05). (**B**) Heat map of downstream gene expression by PID1 overexpression (Threshold: FC>2, *P*<0.05). (**C) and (D)** Bar plot of functional upregulation and downregulation enrichment analysis by GO (PID1_OE_vs_NC). (**E**) Dot plot of signal pathway enrichment analysis by KEGG.

Discussion

PID1 is an intracellular adaptor protein of LDL receptor-associated protein 1 (LRP1), which is associated with lipid metabolism and insulin resistance.[19] PID1 is an intracellular binding protein of LRP1 protein on the cell surface, usually located in the endosome, it can coordinate with LRP1 to regulate the endocytosis of cell membrane lipoproteins[20] and is associated with macrophage phagocytosis in endometriosis.[21] As an anti-cancer gene, PID1 has been reported to have anti-cancer effects in

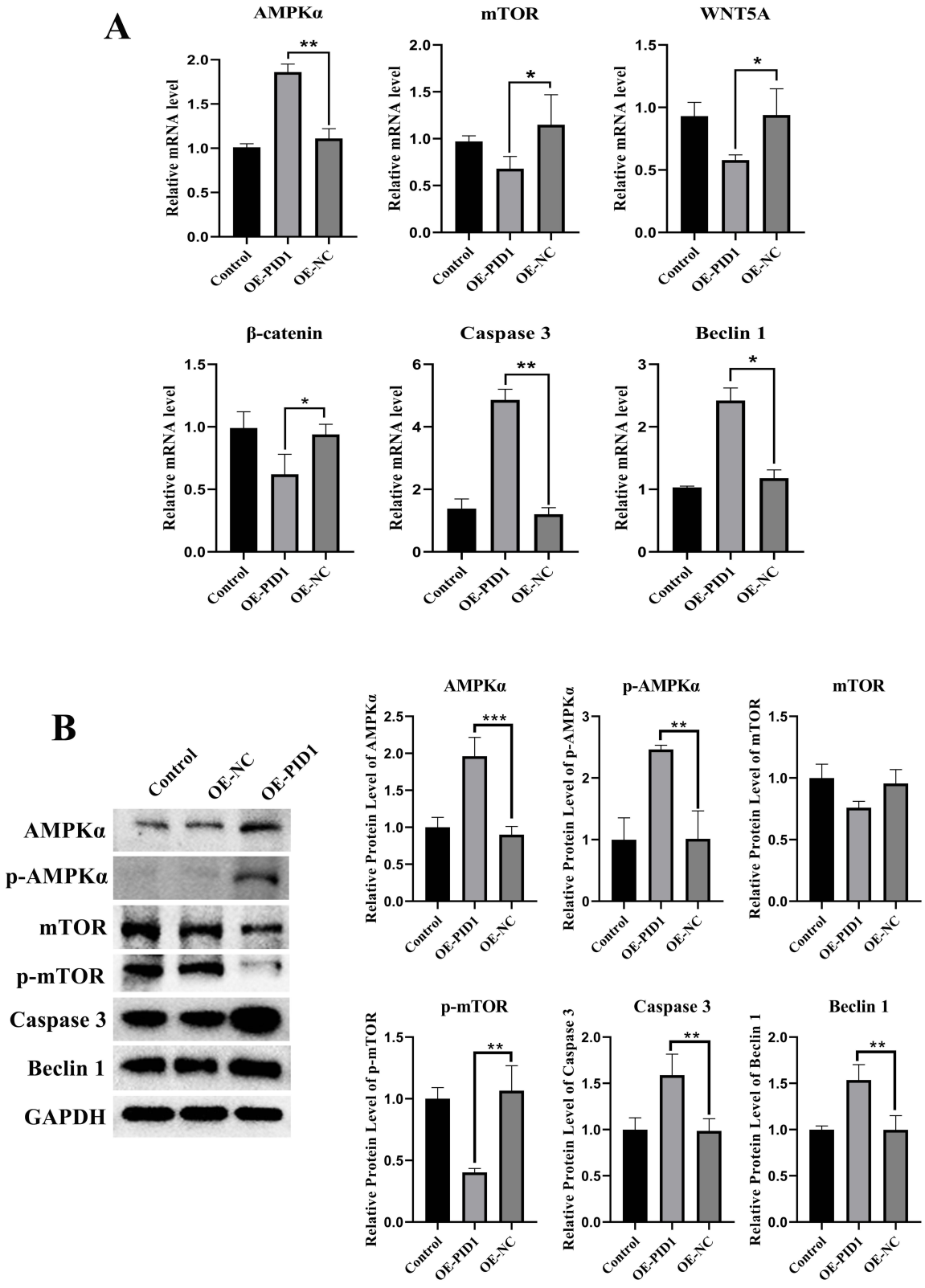

Figure 6 Verify the regulation of PID1 on downstream pathways. **(A)** qPCR was used to detect the expression of AMPKα, mTOR, Wnt5a, β-catenin, Caspase 3, and Beclin 1 mRNA. In the tumor OE-PID1 group, the expression of AMPKα, Caspase 3, and Beclin 1 was increased, while the expression of mTOR, Wnt5a, and β-catenin was decreased (n=3, * *P*<0.05, ** *P*<0.01 versus OE-NC group). (**B**) Western blot was used to detect the expression of AMPKα, p-AMPKα, mTOR, p-mTOR, Caspase 3, and Beclin 1 in the tumor OE-PID1 group. The expression of AMPKα, p-AMPKα, Caspase 3, and Beclin 1 was increased, while that of p-mTOR was decreased (n=3, ** *P*<0.01, *** *P*<0.001 versus OE-NC group).

https://doi.org/10.2147/RRU.S530209

glioma[22] and liver cancer[16] cells. The loss of *PID1* leads to the increase of LRP1 protein on the cell surface.[12] LRP1 can induce M2 polarization of macrophages in bladder cancer to induce anti-PD-1 resistance.[23] Overexpression of PID1 can increase the sensitivity of chemotherapy drugs etoposide and cisplatin in gliomas,[24] and increase the sensitivity of Sorafenib in liver cancer.[16] Therefore, it is believed that low expression of PID1 may promote tumor drug resistance.

This study reported the anti-tumor effect of PID1 in bladder cancer for the first time, mainly through in vitro and in vivo experiments to verify the anti-tumor effect of PID1 in bladder cancer, as well as the expression and function of PID1 in bladder cancer. Clinical prognosis analysis showed a strong association between low expression of PID1 in BLCA patients and adverse clinical outcomes. In vivo tumorigenesis experiments can directly feedback the inhibitory effect of PID1 on tumors, and support PID1 to inhibit bladder cancer in terms of tumor weight and volume. Overexpression of PID1 in RT-112 and SCaBER cells can induce cell cycle arrest in the S phase while reducing cell proliferation and metastasis. As is well known, epithelial-mesenchymal transition (EMT) is closely related to tumor cell invasion and metastasis.[25] Our determination of EMT-related proteins in cells showed that PID1 inhibited the EMT process to a certain extent, thereby inhibiting the metastasis of bladder cancer cells. KEGG enrichment analysis of RNA seq also showed that overexpression and enrichment of PID1 downregulated cell adhesion, cell division, cell migration, and other functions, indicating that PID1 inhibited bladder cancer cells in many ways, and was consistent with our verification of cell function.

At the same time, we validated the downstream signaling pathways potentially regulated by PID1, which promotes AMPK/mTOR pathway activation and inhibits Wnt signaling pathway expression. We focused on validating the universality of AMPK/mTOR. AMPK is an important target for regulating energy metabolism and mitochondrial homeostasis. In many cases, activation of AMPK inhibits aerobic glycolysis, lipid metabolism, and cancer proliferation.[26] The activation of AMPK has been shown to inhibit its downstream target mTOR, which plays a central role in cell growth and proliferation.[27] AMPK can be activated by CaMKK2, while phosphorylated AMPKα2 is located in the Golgi apparatus to promote mitotic fragmentation and regulate the cell cycle.[28] AMPK also induces cell cycle arrest by activating various tumor suppressor factors.[29] Therefore, the effect of PID1 on the cell cycle of bladder cancer may be closely related to AMPK. Secondly, PID1 can also increase the expression of caspase 3 and Beclin 1. As a signaling molecule for apoptosis, caspase 3 can provide feedback on the killing effect of drugs on tumor cells.[30] The process of cell apoptosis is often accompanied by autophagy, and Beclin 1 participates in the entire process of autophagy and plays an important role in regulating the crosstalk between these two types of cell death.[31] The up-regulated expression of Beclin 1 indicates that the PID1-induced apoptosis of bladder cancer cells is accompanied by autophagy. The fusion of large amounts of *SLC2A11–MIF* plays a crucial role in the proliferation and metastasis of BCa by maintaining mRNA stability.[32] SUMO E3 ligase MUL1 inhibits LN metastasis and proliferation in BCa by mediating SUMOylation of HSPA9.[33] The shortcomings of clinical trials have been analyzed, and the small number of clinical samples may result in specificity in the analysis of the results. In the future, we will collect more clinical samples for analysis to eliminate specificity. In vivo experiments on mice were conducted to analyze the role of the *PID1* gene. However, the number of samples is small, and the in-depth analysis of PID1 is not enough. We will test the impact of the *PID1* gene on the Peugeot gene of bladder cancer in subsequent experiments to determine whether it can be used as a therapeutic target.

In conclusion, PID1 is a new tumor suppressor molecule of bladder cancer, which is closely related to the occurrence and development of bladder cancer. The activation of PID1 can significantly inhibit the progression of bladder cancer, providing a new perspective for molecular therapy of bladder cancer. At the same time, PID1 can inhibit the proliferation and metastasis of bladder cancer and promote apoptosis of bladder cancer cells, and may also mediate autophagy of bladder cancer cells and activate the AMPK/mTOR pathway. This study mainly explored the anticancer effect of PID1 at the cellular and animal levels. Although its activation of the AMPK/mTOR pathway has been clarified, the molecular mechanism of PID1's anticancer effect still needs to be further explored. In addition, the relationship between PID1 and the recurrence of bladder cancer is still unclear, which needs further clarification through clinical sample research.

Conclusion

PID1 exhibits a potent inhibitory effect on bladder cancer and activates the AMPK-mTOR signaling pathway to hinder tumor growth.

Acknowledgments

Lingfeng Sun and Chengyi Liu are the first author, responsible for writing the article and data collation. Lin Yuan is the corresponding author and is responsible for revising the article, Yu Cao and Chengyi Liu are responsible for the animal experiments, and Jianghao Li and Lingfeng Sun are responsible for the cell experiments. Thank you all for your help.

Disclosure

No conflict of interest exists in the submission of this manuscript, and the manuscript is approved by all authors for publication. I would like to declare on behalf of my co-authors that the work described is original research that has not been published previously and is not under consideration for publication elsewhere, in whole or in part. All the authors listed have approved the manuscript that is enclosed.

References

1. Dyrskjot L, Hansel DE, Efstathiou JA, et al. Bladder cancer. *Nat Rev Dis Primers*. 2023;9(1):58. doi:10.1038/s41572-023-00468-9
2. Shigeta K, Matsumoto K, Ogihara K, et al. The clinicopathological characteristics of muscle-invasive bladder recurrence in upper tract urothelial carcinoma. *Cancer Sci*. 2021;112(3):1084–1094. doi:10.1111/cas.14782
3. Teoh JY, Kamat AM, Black P C, et al. Recurrence mechanisms of non-muscle-invasive bladder cancer - a clinical perspective. *Nat Rev Urol*. 2022;19(5):280–294. doi:10.1038/s41585-022-00578-1
4. Lopez-Beltran A, Cookson MS, Guercio BJ, et al. Advances in diagnosis and treatment of bladder cancer. *BMJ*. 2024;384:e076743. doi:10.1136/bmj-2023-076743
5. Richters A, Aben KKH, Kiemeney L. The global burden of urinary bladder cancer: an update. *World J Urol*. 2020;38(8):1895–1904. doi:10.1007/s00345-019-02984-4
6. Jubber I, Ong S, Bukavina L, et al. Epidemiology of Bladder Cancer in 2023: a Systematic Review of Risk Factors. *Eur Urol*. 2023;84(2):176–190. doi:10.1016/j.eururo.2023.03.029
7. Chamie K, Litwin MS, Bassett JC, et al. Recurrence of high-risk bladder cancer: a population-based analysis. *Cancer*. 2013;119(17):3219–3227. doi:10.1002/cncr.28147
8. Chen X, Zhang J, Ruan W, et al. Urine DNA methylation assay enables early detection and recurrence monitoring for bladder cancer. *J Clin Invest*. 2020;130(12):6278–6289. doi:10.1172/JCI139597
9. Christensen E, Birkenkamp-Demtroder K, Sethi H, et al. Early Detection of Metastatic Relapse and Monitoring of Therapeutic Efficacy by Ultra-Deep Sequencing of Plasma Cell-Free DNA in Patients With Urothelial Bladder Carcinoma. *J Clin Oncol*. 2019;37(18):1547–1557. doi:10.1200/JCO.18.02052
10. Zambrano N, Minopoli G, Candia DE, et al. The Fe65 adaptor protein interacts through its PID1 domain with the transcription factor CP2/LSF/LBP1. *J Biol Chem*. 1998;273(32):20128–20133. doi:10.1074/jbc.273.32.20128
11. Chen L, Wang XY, Zhu JG, et al. PID1 in adipocytes modulates whole-body glucose homeostasis. *Biochim Biophys Acta Gene Regul Mech*. 2018;1861(2):125–132. doi:10.1016/j.bbagrm.2018.01.001
12. Fischer AW, Albers K, Schlein C, et al. PID1 regulates insulin-dependent glucose uptake by controlling intracellular sorting of GLUT4-storage vesicles. *Biochim Biophys Acta Mol Basis Dis*. 2019;1865(6):1592–1603. doi:10.1016/j.bbadis.2019.03.010
13. Bonala S, Mcfarlane C, Ang J, et al. Pid1 induces insulin resistance in both human and mouse skeletal muscle during obesity. *Mol Endocrinol*. 2013;27(9):1518–1535. doi:10.1210/me.2013-1048
14. Zhang CM, Chen XH, Wang B, et al. Over-expression of NYGGF4 inhibits glucose transport in 3T3-L1 adipocytes via attenuated phosphorylation of IRS-1 and Akt. *Acta Pharmacol Sin*. 2009;30(1):120–124. doi:10.1038/aps.2008.9
15. Erdreich-Epstein A, Robison N, X Ren, et al. PID1 (NYGGF4), a new growth-inhibitory gene in embryonal brain tumors and gliomas. *Clin Cancer Res*. 2014;20(4):827–836. doi:10.1158/1078-0432.CCR-13-2053
16. Yang J, Li S, He J, et al. Dual role of PID1 in regulating apoptosis induced by distinct anticancer-agents through AKT/Raf-1-dependent pathway in hepatocellular carcinoma. *Cell Death Discov*. 2023;9(1):139. doi:10.1038/s41420-023-01405-1
17. Obeidat M, Ding X, Fishbane N, et al. The Effect of Different Case Definitions of Current Smoking on the Discovery of Smoking-Related Blood Gene Expression Signatures in Chronic Obstructive Pulmonary Disease. *Nicotine Tob Res*. 2016;18(9):1903–1909. doi:10.1093/ntr/ntw129
18. Xiong J, Yang L, Deng YQ, et al. The causal association between smoking, alcohol consumption and risk of bladder cancer: a univariable and multivariable Mendelian randomization study. *Int, J, Cancer*. 2022;151(12):2136–2143. doi:10.1002/ijc.34228
19. Yin C, Liu WH, Liu Y, et al. PID1 alters the antilipolytic action of insulin and increases lipolysis via inhibition of AKT/PKA pathway activation. *PLoS One*. 2019;14(4):e0214606. doi:10.1371/journal.pone.0214606
20. Fischer AW, Albers K, Krott LM, et al. The adaptor protein PID1 regulates receptor-dependent endocytosis of postprandial triglyceride-rich lipoproteins. *Mol Metab*. 2018;16:88–99. doi:10.1016/j.molmet.2018.07.010
21. Henlon Y, Panir K, Mcintyre I, et al. Single-cell analysis identifies distinct macrophage phenotypes associated with prodisease and proresolving functions in the endometriotic niche. *Proc Natl Acad Sci U S A*. 2024;121(38):e2405474121. doi:10.1073/pnas.2405474121
22. Han J, Yu X, Wang S, et al. IGF2BP2 Induces U251 Glioblastoma Cell Chemoresistance by Inhibiting FOXO1-Mediated PID1 Expression Through Stabilizing lncRNA DANCR. *Front Cell Dev Biol*. 2021;9:659228. doi:10.3389/fcell.2021.659228
23. Du Y, Liu Y, Cao J, et al. LDL receptor related protein 1 is an adverse prognostic biomarker that correlates with stromal remodeling and macrophages infiltration in bladder cancer. *Front Immunol*. 2023;14:1113756. doi:10.3389/fimmu.2023.1113756
24. Xu J, Ren X, Pathania AS, et al. PID1 increases chemotherapy-induced apoptosis in medulloblastoma and glioblastoma cells in a manner that involves NFkappaB. *Sci Rep*. 2017;7(1):835. doi:10.1038/s41598-017-00947-6
25. Wrighton KH. Cell migration: EMT promotes contact inhibition of locomotion. *Nat Rev Mol Cell Biol*. 2015;16(9):518. doi:10.1038/nrm4045

26. Herzig S, Shaw RJ. AMPK: guardian of metabolism and mitochondrial homeostasis. *Nat Rev Mol Cell Biol*. 2018;19(2):121–135. doi:10.1038/nrm.2017.95
27. Huang Y, Zhou S, He C, et al. Phenformin alone or combined with gefitinib inhibits bladder cancer via AMPK and EGFR pathways. *Cancer Commun*. 2018;38(1):50. doi:10.1186/s40880-018-0319-7
28. Fogarty S, Rosss FA, VARA CIRUELOS D, et al. AMPK Causes Cell Cycle Arrest in LKB1-Deficient Cells via Activation of CAMKK2. *Mol Cancer Res*. 2016;14(8):683–695. doi:10.1158/1541-7786.MCR-15-0479
29. Hsu CC, Peng D, Cai Z, et al. AMPK signaling and its targeting in cancer progression and treatment. *Semin Cancer Biol*. 2022;85:52–68. doi:10.1016/j.semcancer.2021.04.006
30. Bhat AA, Thapa R, Afzal O, et al. The pyroptotic role of Caspase-3/GSDME signalling pathway among various cancer: a Review. *Int J Biol Macromol*. 2023;242(Pt 2):124832. doi:10.1016/j.ijbiomac.2023.124832
31. Ma Q, Yu J, Zhang X, et al. Wnt/beta-catenin signaling pathway-a versatile player in apoptosis and autophagy. *Biochimie*. 2023;211:57–67. doi:10.1016/j.biochi.2023.03.001
32. Cheng L, Yang C, Lu J, et al. Oncogenic SLC2A11-MIF fusion protein interacts with polypyrimidine tract binding protein 1 to facilitate bladder cancer proliferation and metastasis by regulating mRNA stability. *MedCom*. 2024;5(9):e685. doi:10.1002/mco2.685
33. Wu J, Huang M, Dong W, et al. SUMO E3 ligase MUL1 inhibits lymph node metastasis of bladder cancer by mediating mitochondrial HSPA9 translocation. *Int J Biol Sci*. 2024;20(10):3986–4006. doi:10.7150/ijbs.98772